

Atomistic understanding of diffusion kinetics in nanocrystals from molecular dynamics simulationsYun-Jiang Wang,^{1,*} Guo-Jie J. Gao,² and Shigenobu Ogata^{2,1,†}¹*Center for Elements Strategy Initiative for Structural Materials (ESISM), Kyoto University, Sakyo, Kyoto 606-8501, Japan*²*Graduate School of Engineering Science, Osaka University, Osaka 560-8531, Japan*

(Received 21 May 2013; revised manuscript received 24 August 2013; published 9 September 2013)

Understanding the grain size effect on diffusion in nanocrystals has been hampered by the difficulty of measuring diffusion directly in experiments. Here large-scale atomistic modeling is applied to understand the diffusion kinetics in nanocrystals. Enhanced short-circuit diffusivity is revealed to be controlled by the rule of mixtures for grain-boundary diffusion and lattice diffusion, which can be accurately described by the Maxwell-Garnett equation instead of the commonly thought Hart equation, and the thermodynamics of pure grain-boundary self-diffusion is not remarkably affected by varying grain size. Experimentally comparable Arrhenius parameters with atomic detail validate our results. We also propose a free-volume diffusion mechanism considering negative activation entropy and small activation volume. These help provide a fundamental understanding of how the activation parameters depend on size and the structure-property relationship of nanostructured materials from a physical viewpoint.

DOI: 10.1103/PhysRevB.88.115413

PACS number(s): 66.30.Pa, 66.30.Fq, 66.30.Xj, 61.72.Mm

I. INTRODUCTION

There are two types of atomic diffusion in polycrystalline solids: diffusion in the lattice and diffusion in lattice defects such as dislocations, grain boundaries (GBs), and surfaces.^{1,2} The latter is sometimes called the high-diffusivity path, or short-circuit diffusion path, because usually the diffusivities in such defects are much higher than that in the lattice.¹ Among them, GB diffusion is the most important for the high-temperature stability of polycrystals since it is directly related to processes such as creep,^{3,4} grain growth, and recrystallization,⁵⁻⁷ superplasticity,⁸ and sintering.¹ In particular, in nanocrystalline (NC) metals, which are polycrystals whose grain size is smaller than several hundred nanometers, GB diffusion exerts a significant influence on macroscopic mechanical properties since the volume fraction of GBs drastically increases with decreasing grain size.^{9,10} It is well accepted that the diffusion kinetics usually follows an Arrhenius type of temperature dependence:

$$D = D_0 \exp\left(-\frac{\Delta Q}{k_B T}\right), \quad (1)$$

where D is the diffusion coefficient, D_0 is a pre-exponential factor, ΔQ is the activation energy, k_B is Boltzmann's constant, and T is the absolute temperature. In the case of face-centered-cubic metals such as copper, the activation energy of lattice diffusion is about twice that of GB diffusion.¹¹⁻¹³ The effective diffusivity of NC copper is greatly enhanced compared with its conventional coarse-grained counterpart.¹³ However, quantitative knowledge on pure GB diffusivity in polycrystalline metals is still controversial, because we do not have enough experimental data with different grain sizes and, moreover, the grain size of these polycrystalline metals is sometimes not well controlled. Therefore, we have not yet reached a well-established framework for the size dependence of diffusion kinetics in polycrystalline metals, such as GB diffusion-accommodated Coble creep and GB sliding creep,^{3,4} which are fundamental to understanding the inverse Hall-Petch scaling in NC metals.^{9,10}

With advances in computer capacity and the development of reliable interatomic potentials, atomistic modeling enables us to predict experimentally comparable diffusivity in the temperature range of $[0.6T_m, T_m]$, where T_m is the melting point.¹⁴⁻²¹ Besides molecular dynamics (MD), kinetic Monte Carlo also permits accurate calculations of diffusivity.^{15,19} However, it is only effective if the elementary diffusion steps can be defined previously.¹⁹ Therefore, in this study we simply carry out MD for the calculations of diffusivity of nanocrystals which may include general disordered GBs. The present modeling aims at addressing several important unknowns: (1) Does the enhancement of diffusivity in NC metals come from the variation in activation parameters, or does it come from other size-dependent factors? (2) Since NC metals are actually a mixed pack of nanosized crystallites and disordered GB regions, what is the rule of mixtures behind diffusivity? (3) What is the microscopic mechanism of short-circuit GB diffusion? Is it a mechanism with dominating contributions from vacancies or interstitial atoms, or is it a concept of excess free volume?²²

II. METHODOLOGY

The modeling of diffusion kinetics is performed on fully dense three-dimensional (3D) NC copper with grain size ranging 5–15 nm, which is commonly thought to be within the inverse Hall-Petch regime.^{9,10} Diffusional mechanisms such as GB diffusion and its related GB migration and sliding become dominant at such a small scale. The 3D nanocrystal is built based on a Voronoi algorithm in which grain seeds are previously determined according to random close packing of monodisperse hard spheres,²³ which ensures a $3 \times 3 \times 3$ mesh of almost equally sized grains; an example of a 15-nm-grain-sized sample shown in Fig. 1(a). All the grains are randomly oriented. However, we fix those orientations when the grain size of the NC model is varied. The biggest model, with a grain size of 15 nm (and a sample size of about $45 \times 45 \times 45 \text{ nm}^3$), contains about 7 540 000 atoms. In the present study, we ignore the variation of GB types with change

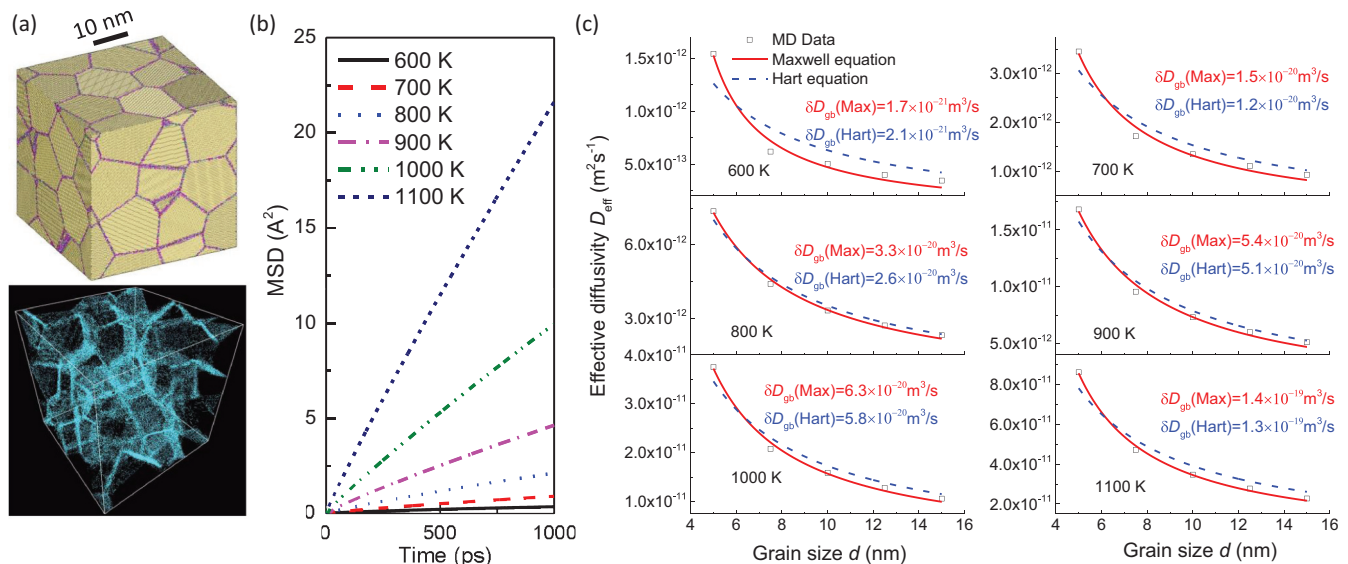


FIG. 1. (Color online) Short-circuit diffusion in NC copper. (a) Upper: NC copper sample with $3 \times 3 \times 3$ grains and grain size $d = 15$ nm. Lower: 3D view of fast diffusion channels; see Supplemental Material for a movie with a 360° perspective (Ref. 32). Only those atoms that have traveled farther than 0.6 nm after 1 ns are displayed. (b) MSD vs time at different temperatures with $d = 10$ nm. (c) Effective diffusion coefficient vs d at different temperatures. Red solid lines and blue dash lines denote those fits to the Maxwell-Garnett equation and the Hart equation, respectively. δD_{gb} from fitting is displayed for each temperature.

in grain size. Therefore, the conclusions are applicable for those high-angle GBs generated by the Voronoi tessellation polycrystalline generator with random crystal orientation setting.

MD simulations are performed using the embedded-atom method (EAM) potential,²⁴ which is implemented on the large-scale atomic/molecular massively parallel simulator (LAMMPS).²⁵ This potential is reliable for predicting accurate information for diffusion processes, and the migration energy of point defects. It has been widely used to study the diffusion behaviors of various GBs,^{16,17,19} GB triple junctions,¹⁸ and diffusion-induced GB mobilities.^{5,20} Here the diffusion kinetics in NC copper is investigated over a wide temperature range of 600–1100 K. Before measuring the diffusivity, all the samples are thermally equilibrated for 100 ps at each specific targeted temperature by using a Nosé-Hoover thermostat within an NPT ensemble,²⁶ where N , P , and T denote the number of atoms, hydrostatic pressure, and absolute temperature, respectively. A Parrinello-Rahman technique is used to control the hydrostatic pressure during thermal relaxation and derivation of the activation volume.²⁷ Then a MD simulation is performed for each model for 1 ns, which allow us to reach the effective diffusion coefficient, $D_{\text{eff}} = \frac{\langle |\mathbf{r}(t) - \mathbf{r}(0)|^2 \rangle}{6t}$, where $\mathbf{r}(t)$ and $\mathbf{r}(0)$ are the positions of atoms at times t and $t = 0$, respectively. This is actually the well-known Einstein relation. The mean-squared displacement (MSD) $\langle |\mathbf{r}(t) - \mathbf{r}(0)|^2 \rangle$ is shown as a function of time at different temperatures in Fig. 1(b) in the case of $d = 10$ nm. The slopes of these well-defined linear relations actually provide quantitative information for the diffusion coefficients. The diffusivities are determined by the relation of MSD against time after 500 ps, where a linear relation has been well established.

III. RESULTS AND DISCUSSION

A. Rule of mixtures

It is frequently discovered that diffusivity is pronouncedly enhanced by reducing the grain size of a polycrystal.¹³ However, the atomic mechanism underlying this ubiquitous phenomenon is still poorly understood. For example, we are not clear how the diffusion activation energy varies with change in grain size nor how it can affect the polycrystal diffusivity. Smaller activation energy leads to faster diffusion according to the Arrhenius equation (1). Besides the variation in activation energy, another possible diffusion-enhancing mechanism is related to the rule of mixtures (ROM) for diffusion kinetics in polycrystalline materials, which involves (the different roles of) lattice diffusion and GB diffusion.¹ In the present study we highlight atomistic modeling toward a concrete understanding of pure self-diffusion of NC metal; in particular, we are interested in the grain size dependence of diffusivity.

The effective self-diffusivity in a polycrystal depends strongly on the arrangement of grains and GBs. It is intuitive to assume that the upper limit of the effective diffusivity involves the parallel arrangement of these two counterparts along the diffusion direction. The upper limit of the effective diffusivity in a polycrystal is described by the Hart equation²⁸

$$D_{\text{eff}}(d) = gD_{\text{gb}} + (1 - g)D_{\text{l}}, \quad (2)$$

where g is the volume fraction of GBs in the polycrystal, approximately $\frac{3\delta}{d}$, with δ the width of the grain boundary, which has been estimated to be of the order of 0.5 nm in the present models (an estimation that is in agreement with experimental findings²⁹); $D_{\text{gb}} = D_{\text{gb0}} \exp(-\frac{\Delta Q_{\text{gb}}}{k_B T})$ is the pure GB diffusion coefficient, with D_{gb0} and ΔQ_{gb} its corresponding

pre-exponential factor and activation energy, respectively; and the lattice diffusion coefficient $D_1 = D_{10} \exp(-\frac{\Delta Q_1}{k_B T})$ denotes the crystallite diffusivity, with the formula adopting similar definitions as that of GB diffusion. In general, the GB self-diffusion coefficient is much larger than that of lattice diffusion: namely, $D_{gb} \gg D_1$. For example, the activation energy of self-diffusion in nano- and single-crystalline copper were reported to be 62 and 191 kJ/mol, respectively.¹³ Consequently, their self-diffusion coefficients were measured to be, respectively, 2.6×10^{-20} and 4×10^{-40} m²/s at ambient temperature.¹³ There exists a difference of approximately 20 orders of magnitude in self-diffusion between nano- and single-crystalline copper.

In contrast with the upper limit, the lower limit of effective diffusivity in a polycrystal involves a serial arrangement of grains and GBs along the direction of diffusion. It is formulated as¹

$$D_{\text{eff}}(d) = \frac{D_{\text{gb}} D_1}{g D_{\text{gb}} + (1 - g) D_1}. \quad (3)$$

In this way, the effective diffusivity of a polycrystal is treated as that of a single crystal. The diffusion carriers have to overcome mainly the energy barriers in the crystallite lattice, which leads to slow diffusion. Therefore, it is precluded as a fast-diffusion mechanism in NC metals.

However, diffusion in a real polycrystal should be neither of parallel nor serial arrangement of GBs and grains. In 3D polycrystals, the Maxwell-Garnett equation

$$D_{\text{eff}}(d) = \frac{D_{\text{gb}} [2g D_{\text{gb}} + (3 - 2g) D_1]}{(3 - g) D_{\text{gb}} + g D_1} \quad (4)$$

has been proposed to be an approximation of the effective diffusivity.³⁰ However, no evidence of atomic fidelity detail has been available to our best knowledge.

The lower graph in Fig. 1(a) highlights the 3D short-circuit diffusion paths in the case of NC copper with grain size $d = 15$ nm. We visualize this structure by selecting those atoms whose traveled distance is greater than 6 Å after 1-ns diffusion at 800 K, and the visualization is done with ATOMEYE.³¹ It is noteworthy that the highlighted skeleton frame reproduces the polyhedral GB structures, which clearly verifies that fast diffusion occurs only in GBs of NC copper from atomic level information. For 3D diffusion channels from a 360° perspective the reader is referred to Movie S1 in the Supplemental Material.³² If $D_{\text{gb}} \gg D_1$ and the volume fraction of GB regions becomes substantial, Eqs. (2) and (4) are reduced to

$$D_{\text{eff}}(d) \approx g D_{\text{gb}} = \frac{3\delta}{d} D_{\text{gb}} \quad (5)$$

and

$$D_{\text{eff}}(d) \approx \frac{2g}{3-g} D_{\text{gb}} = \frac{2\delta}{d-\delta} D_{\text{gb}}. \quad (6)$$

Here we do not discuss Eq. (3) since it sets the lower limit of effective diffusivity, and it requires the most contribution from only lattice diffusion, which is not applicable in the present case of short-circuit diffusion.

In the present study, we would like to provide atomistically resolved detail to confirm which approximation can well describe the dependence of size upon diffusivity in NC metals.

Figure 1(c) summarizes the effective diffusivity as a function of grain size. The results are plotted at different temperatures from 600 to 1100 K. The dashed blue and red solid lines denote those curves that are fitted to Eqs. (5) and (6), respectively. It is noted that the plots at 600 and 700 K are not reliable since there is an overestimation of diffusivities. The MSD at such low temperature has not yet reached a steady state with the short MD time scale. Therefore, our conclusions are based on the results derived at temperatures above 800 K. It is clear that the Maxwell-Garnett equation is a better approximation of the effective diffusivity compared with the Hart equation. A similar conclusion has been reached with Monte Carlo simulations.³³ However, here we furthermore provide atomic scale evidence without the inherent assumptions embedded in Monte Carlo modeling. The Hart equation is usually assumed during the derivation of the constitutive equations for creep governed by GB diffusion³ and its accommodating GB sliding and migration.⁴ The Hart equation leads to an $\dot{\epsilon} \propto d^{-3}$ relationship for the strain rate dependence on size for Coble and GB sliding creep. Usually, this is a sound approximation provided that other degrees of freedom (including activation entropy, attempt frequency, and unit strain^{3,4}) can be manipulated. However, the relationship could be revised according to the more reasonable approximation illustrated by Eq. (6) instead of Eq. (5). In the next section, the activation parameters will be evidenced to be insensitive to grain size. Thus the enhanced diffusivity of NC metals is mainly attributed to the ROM, which is presented by Eq. (6). It is noted that the triple junctions are generally the fastest diffusion channels in nanocrystals (see Supplemental Material³²). Chen and Schuh have developed a composite model to describe the effective diffusivity of the polycrystal by considering various structural defects, i.e., grain boundaries, triple junctions, and also dislocations.³⁴ They find that triple junction diffusion is relevant at small size scale. However, here we do not separate the diffusivity of the triple junction from the general GB diffusion. The difference in diffusivities of the triple junctions and that of general GBs has been shown to be not significant enough to require a new diffusion regime.¹⁸ Therefore, the conclusion about the rule of mixtures does not change if we assume the triple junction diffusion and GB diffusion as a general intergranular diffusion. It is a future study to find the detailed ROMs about GB and triple junction diffusion.

B. Size dependence of activation parameters

The diffusion kinetics follows an Arrhenius relation between diffusion coefficient and temperature, as illustrated by Eq. (1). According to the Gibbs-Helmholtz relation, the effective activation energy ΔQ_{eff} of diffusion can be reached as

$$\Delta Q_{\text{eff}}(d) = -\frac{\partial \ln D_{\text{eff}}(d)}{\partial (1/k_B T)}. \quad (7)$$

Modeling results and experimental data for effective diffusivity are plotted in Fig. 2. The diffusivity presents an Arrhenius relation against reciprocal temperature. We only show two examples here, for grain sizes of 7.5 and 15 nm. In the former case, the experiment is performed on a similar grain size of about 8 nm,¹¹ whereas, in the latter case, the experimental diffusivity is reduced from samples with larger grain size of about 300 nm³⁵ and about 120 nm.³⁶ These data

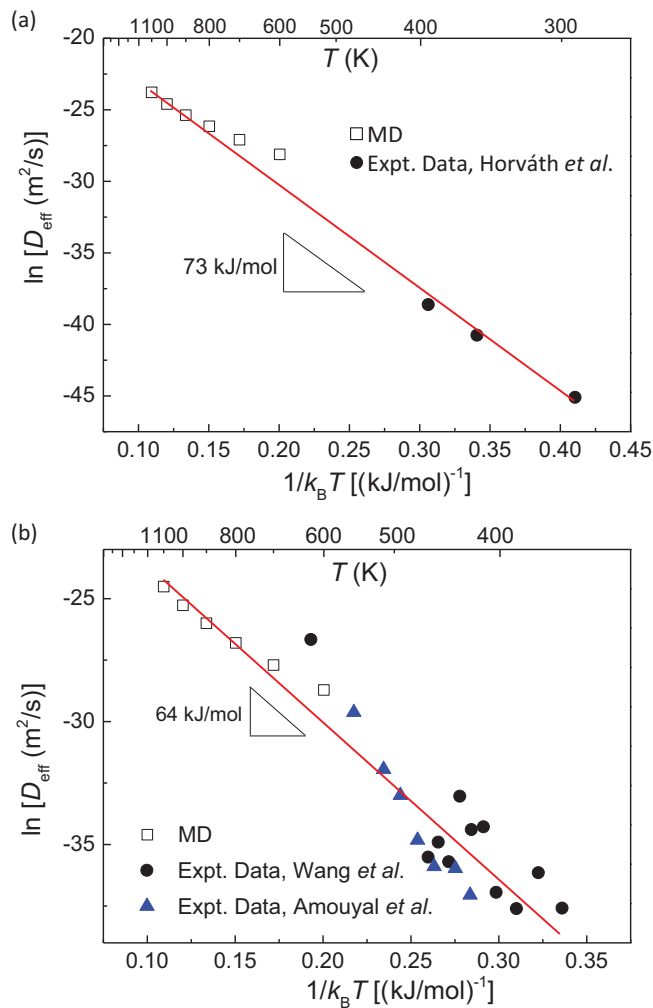


FIG. 2. (Color online) Arrhenius plot of effective self-diffusion in NC copper with grain size of (a) 7.5 nm and (b) 15 nm. Open and solid symbols stand for the present modeling and experimental data, respectively. The latter presented in (b) are reduced to the case of grain size of 15 nm according to the Maxwell-Garnett equation [Eq. (6)]. Linear fits are based on experimental data along with the modeling data above 800 K.

are normalized to NC copper with a grain size of 15 nm according to Eq. (6). It is noted that both modeling and experiment results follow a similar linear relation, except for those modeling data that lie at lower temperatures of 600 and 700 K. The temperature range 800–1100 K is reliable for predicting an experimentally comparable diffusivity according to the plot in Fig. 2. According to the data over the whole temperature range, the activation energies are fitted to be 71 and 64 kJ/mol for samples with grain sizes of $d = 7.5$ and $d = 15$ nm, respectively. Such data are in excellent agreement with experimental measurements.^{11–13,35–39} Furthermore, if we fit the activation energy by only taking account of the temperature range 800–1100 K, the modeling predicts activation energies of 57.3 and 55.3 kJ/mol for $d = 7.5$ and $d = 15$ nm, respectively. The corresponding experimental data are 61.7 kJ/mol¹¹ and 57 kJ/mol,³⁶ respectively. The fits based on the temperature range 800–1100 K lead to activation energies with better agreement to experiments, and more

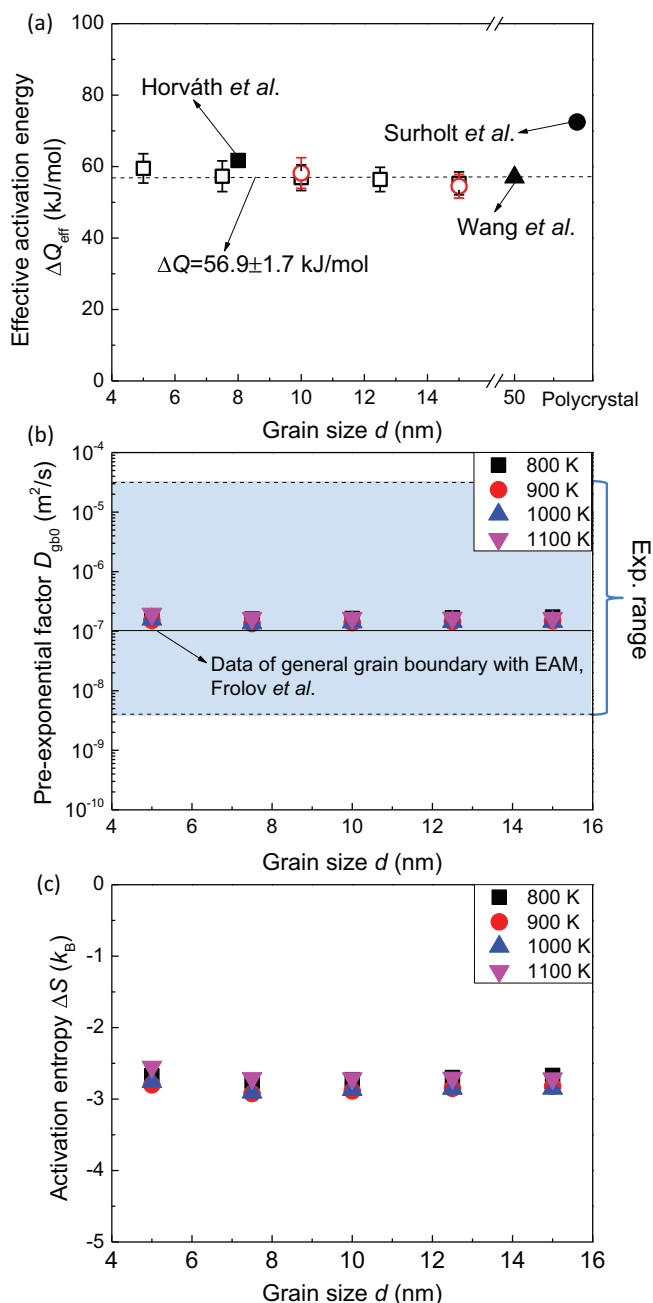


FIG. 3. (Color online) Size dependence of activation parameters. (a) Effective activation energy, (b) pre-exponential factor, and (c) activation entropy. The dashed line in (a) indicates an average value of the modeling data. The shaded area in (b) denotes the scattered range of reported experimental data, and the solid line implies the magnitude of the prefactor from other modelings on a general high-angle GB with the same EAM potential.

importantly there exists good linear relation on the Arrhenius plot. Therefore, all the activation energies in this study are according to this temperature range.

To derive further understanding of the enhanced diffusivity upon the reduction in grain size, we should first derive the relationship for how activation energy depends on size according to Eq. (1). The effective activation energy ΔQ_{eff} is shown in Fig. 3(a) as a function of grain size. ΔQ_{gb} is

not sensitive to the variation in grain size, which stays near an average value of about 57 kJ/mol and agrees well with not only experimental data but also MD simulations on other general high-angle GBs, as shown in Refs. 16–18. We should note that activation energy is quite sensitive to the geometry of the GBs. It can be as small as 50 kJ/mol or as large as 250 kJ/mol depending on the local interface structures.^{16,17} When we change the grain size of the NC model, the orientations that connect neighboring grains are fixed.

Based on knowledge of the activation energy and the ROM as shown in Eq. (6), the pre-exponential factor of pure GB diffusion D_{gb0} can be determined. It is a prefactor for GB diffusion that already excludes the size effect arising from the ROM. The result, plotted in Fig. 3(b), is almost a constant and is not sensitive to either temperature or grain size. The average value of D_{gb0} is determined to be about 1.6×10^{-7} m²/s, which agrees with a previous MD modeling result of $(1.0 \pm 0.2) \times 10^{-7}$ m²/s for general high-angle GBs.

So far, both the activation energy and the pre-exponential factor of pure GB diffusion have been verified to be independent of grain size. Thus, the GB self-diffusivity itself is not size sensitive. Therefore, pure GB diffusivity can be correlated to effective diffusivity via a parameter that is determined by grain size, as shown in Eq. (6). In terms of Eq. (6), the activation energy of GB diffusion, ΔQ_{gb} , can be derived directly from the effective diffusivity $D_{\text{eff}}(d)$, i.e., $\Delta Q_{gb} \approx -\frac{\partial \ln D_{\text{eff}}(d)}{\partial (1/k_B T)}$, instead of turning back to pure GB diffusivity D_{gb} , provided that the grain size is fixed and that the variation of GB width with temperature is negligible. Consequently, we conclude that the enhanced diffusivity of NC metal originates from the ROM, which is expressed by the reduced Maxwell-Garnett equation [Eq. (6)], instead of the usual idea that fast diffusion originates from the variation in activation parameters.^{1,13} We note that here we assume that the GB characters do not change with variation in grain size. Therefore, the lack of dependence of grain size effect on the diffusion kinetics of polycrystalline models may be a reflection of our methodology for creating the GBs. It needs further work to verify whether GB characters and kinetics change with grain size.

If the pre-exponential factor of pure GB diffusion is size independent, then the activation entropy, which is included in this factor, should also be expected to be a constant value regardless of variation in grain size. Without external pressure, the GB diffusivity can be written as¹

$$D_{gb} = f\gamma\delta^2\nu_0 \exp\left(\frac{\Delta S}{k_B}\right) \exp\left(-\frac{\Delta Q_{gb}}{k_B T}\right), \quad (8)$$

from a physical perspective. Here f is a correlation factor, and γ is a geometrical factor. They are both on the order of unity, and here we take $f\gamma = 1$ for simplicity.¹ δ is originally the jump distance of the diffusion carrier; here we assume it to be of the order of the GB width, which is estimated to be 0.5 nm in the present models. This magnitude is in agreement with experimental observations.²⁹ ν_0 is the atomic vibrational frequency and is of the order of 10^{13} s⁻¹ to a first approximation. Therefore, the activation entropy ΔS can be predicted with knowledge of D_{gb} and ΔQ_{gb} , which have been provided by our MD simulations. The derived activation entropy is shown in Fig. 3(c) as a function of grain size.

ΔS is size insensitive. It is estimated to be of the order of $-2k_B$ to $-3k_B$. This value contains contributions from the formation entropy and migration entropy of defects. It has been reported that the formation entropy of point defect in GBs is on the order of several k_B .^{15–17} Therefore, the migration entropy should be more negative but remains of the same order. Moreover, the width of GBs generally increases with increasing temperature. This trend leads to a more negative activation entropy according to Eq. (8). However, the negative character of activation entropy does not change with any reasonable choice of δ .

The activation entropy arises from an anharmonic effect when the diffusion carrier moves from the equilibrium position to the transition state. For a qualitative understanding, we note that the harmonic transition state approximation correlates activation entropy to vibration frequency by $\nu_0 \exp(\Delta S/k_B) = \prod_{i=1}^{3N} \nu_i^{\text{initial}} / \prod_{i=1}^{3N-1} \nu_i^{\text{saddle}}$, where ν_i^{initial} and ν_i^{saddle} are the vibrational frequency of the i th normal modes at the local energy minimum and the saddle point state in the $3N$ -dimensional configurational space, respectively. There are two possible diffusion mechanisms. One involves the migration of a unit vacancy. This mechanism requires a vacancy migration that is of the size of unit atomic volume with the help of several neighboring atoms. Mantina *et al.* have shown a positive entropic contribution to the self-diffusion of Al by a first-principles calculation.⁴⁰ They find that most of the normal model frequencies shift to lower values at the saddle point compared with the initial stable state. Therefore, they conclude that there is a positive entropic effect on vacancy migration. The other diffusion mechanism involves the migration of interstitial atoms.⁴⁰ This interstitial diffusion opens smaller spaces during migration compared with vacancy diffusion. Equivalently, it could be assumed to act as excess free-volume diffusion, in which the volume of the diffusion carrier is smaller than that of the vacancy. The vibrational state is more constrained when the migrating interstitial atom approaches the saddle point compared with the stable state, leading to an increase in the vibration frequency of the saddle state. Consequently, the activation entropy is anticipated to be negative.⁴¹ Milman *et al.* have verified a negative entropy of interstitial diffusion in crystalline silicon by using a combined thermodynamical integration and first-principles MD method.⁴¹ In summary, the sign of the activation entropy presumably provides an indication of the diffusion mechanism. However, further study is needed to verify the interrelation between the activation entropy and the diffusion mechanism, in particular in the case of GB diffusion.

C. Mechanism of GB diffusion

A comprehensive characterization of diffusion kinetics requires complete information on three important activation parameters, i.e., energy, entropy, and volume of activation. Among them, the activation volume is commonly thought to be an intuitive indication of the diffusion mechanism.¹⁰ To derive it, we apply hydrostatic pressure with varying magnitude up to 0.4 GPa to a sample with a grain size of 10 nm. In general, the activation volume is a tensor with anisotropic characteristics.¹⁰ However, it is found that its shear components are negligible compared with its tensile components.¹⁰ In the present case

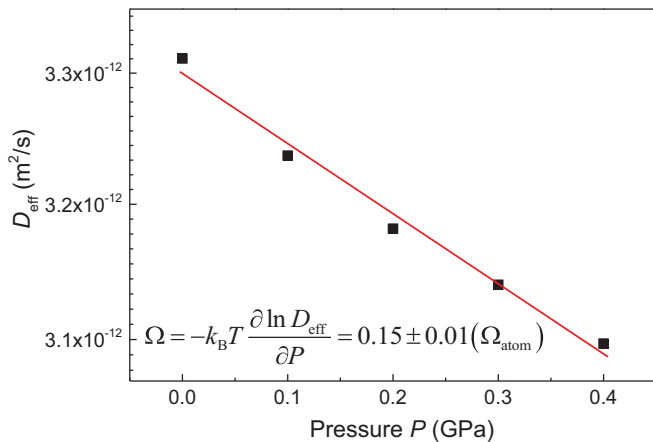


FIG. 4. (Color online) Pressure dependence of effective GB self-diffusion (on a natural logarithmic scale) of NC copper with grain diameter of 10 nm at 800 K. The slope leads to an activation volume of the order of 0.15 atomic volume.

of GB diffusion, we use the hydrostatic pressure since the atoms in the GBs are disordered, and the activation volume is assumed to be isotropic. A characteristic value for the activation volume can be reached through this strategy. In the presence of external pressure P , the GB diffusivity is correlated to the activation enthalpy $\Delta H_{\text{gb}} = \Delta Q_{\text{gb}} + P\Omega$ via

$$D_{\text{gb}} = D_{\text{gb}0} \exp\left(-\frac{\Delta Q_{\text{gb}} + P\Omega}{k_{\text{B}}T}\right), \quad (9)$$

where Ω is the activation volume of GB diffusion. If the pre-exponential factor $D_{\text{gb}0}$ is not sensitive to pressure, one can obtain the activation volume through the following expression:

$$\Omega = -k_{\text{B}}T \frac{\partial \ln D_{\text{eff}}}{\partial P}, \quad (10)$$

where we can use straightforwardly the effective diffusivity D_{eff} instead of pure GB diffusivity D_{gb} because they are only differentiated by a constant at a given grain size according to Eq. (6).

In Fig. 4 we present a natural logarithmic plot of D_{eff} versus the magnitude of applied pressure. The gradient of this well-defined linear relation leads to an activation volume of the order of magnitude of $0.15\Omega_{\text{atom}}$ via Eq. (10), in which the unit Ω_{atom} denotes the volume of a Cu atom in the perfect fcc lattice (about 11.8 \AA^3). Small activation volume means that the influence of pressure on the diffusivity is not substantial in the pure GB self-diffusion of NC copper. The calculated data here are much smaller than the activation volume of vacancy diffusion in fcc Cu, which can be determined either from calculation with the same EAM potential¹⁰ or experimental measurement.¹ The reported activation volume for lattice diffusion is on the order of Ω_{atom} .^{1,10} The lattice diffusion mechanism is well established by a vacancy migration process. Consequently, vacancy migration cannot be a reasonable mechanism for GB diffusion. Moreover, a small activation volume is in contrast with an atomistic simulation of diffusional creep on NC copper, in which the activation volume is found to be as much as several times the atomic volume.⁴²⁻⁴⁴ The reason for this difference is that creep simulations have been done by applying uniaxial stress, which could activate and effectively drive the more

collective components of GB activity, such as GB sliding and migration, which involve simultaneous participation of multiple atoms.¹⁰

We have mentioned an excess free-volume diffusion mechanism in the discussion of activation entropy. The diffusion carrier (free volume) can be smaller than the volume of the atom. Small-free-volume diffusion needs only neighboring atoms to open tiny spaces, in contrast with vacancy migration, which requires a neighbor atom of the vacancy to occupy its original position. Therefore, the activation volume is expected to be only a small proportion of the atomic volume for free-volume diffusion but roughly one atomic volume for vacancy mechanism.² In the present case of small activation volume, it is more likely to be a free-volume mechanism that accommodates GB diffusion. This hypothesis is also supported by the previously mentioned negative entropy shown in Fig. 3(c). The conclusion seems to be self-consistent in the language of both vibrational entropy and geometrical analysis of activation volume. In a recent study, Bachurin *et al.* have proposed the concept of free-volume migration to explain the elastic and plastic anisotropy after straining of NC palladium.²²

IV. SUMMARY

We have provided a report on the size dependence of diffusion kinetics of NC metal with atomic details. Atomically resolved information enables us to reveal several important unknowns related to GB self-diffusion: (1) The enhanced diffusivity of NC metal is caused by a ROM for pure GB diffusion and lattice diffusion, whereas pure GB diffusion kinetics is not obviously size dependent. The activation parameters of the Arrhenius relation from our modelings are in agreement with experimental data, indicating that the physics of GB diffusion can be captured within the approachable MD time window. (2) The Maxwell-Garnett model, in which one considers the 3D arrangement of GBs and the grain interior, is confirmed to be an accurate approximation of effective diffusivity of NC metals rather than the commonly used Hart approximation. The latter is usually assumed in the constitutive equations for creep governed by GB diffusional mechanisms. (3) Negative activation entropy and small activation volume consistently indicate a free-volume migration mechanism of GB diffusion in NC metals. We hope that our findings and the discussion herein will expand our understanding of the size dependence and the diffusion mechanism of NC metals with atomic detail. The reported size effect on diffusion potentially sheds light on building a physically sound strength-size scaling law in the inverse Hall-Petch regime.

ACKNOWLEDGMENTS

This work was partially supported by the Elements Strategy Initiative for Structural Materials (ESISM), Scientific Research on Innovative Area ‘‘Bulk Nanostructured Metals’’ (Grant No. 22102003), Scientific Research (A) (Grant No. 23246025), Challenging Exploratory Research (Grant No. 25630013), and JST under Collaborative Research Based on Industrial Demand (Heterogeneous Structure Control).

*yjwang@me.es.osaka-u.ac.jp

†ogata@me.es.osaka-u.ac.jp

- ¹H. Mehrer, *Diffusion in Solids: Fundamentals, Methods, Materials, Diffusion-Controlled Processes*, Springer Series in Solid-State Sciences Vol. 155 (Springer, London, 2007).
- ²I. Kaur, Y. Mishin, and W. Gust, *Fundamentals of Grain and Interphase Boundary Diffusion* (Wiley, Chichester, 1995).
- ³R. L. Coble, *J. Appl. Phys.* **34**, 1679 (1963).
- ⁴H. Lüthy, R. A. White, and O. D. Shereby, *Mater. Sci. Eng.* **39**, 211 (1979).
- ⁵A. Karma, Z. T. Trautt, and Y. Mishin, *Phys. Rev. Lett.* **109**, 095501 (2012).
- ⁶C. E. Krill III, L. Helfen, D. Michels, H. Natter, A. Fitch, O. Masson, and R. Birringer, *Phys. Rev. Lett.* **86**, 842 (2001).
- ⁷D. Farkas, S. Mohanty, and J. Monk, *Phys. Rev. Lett.* **98**, 165502 (2007).
- ⁸M. F. Ashby and R. A. Verrall, *Acta Metall.* **21**, 149 (1973).
- ⁹M. A. Meyers, A. Mishra, and D. J. Benson, *Prog. Mater. Sci.* **51**, 427 (2006).
- ¹⁰T. Zhu and J. Li, *Prog. Mater. Sci.* **55**, 710 (2010).
- ¹¹J. Horváth, R. Birringer, and H. Gleiter, *Solid State Commun.* **62**, 319 (1987).
- ¹²S. Schumacher, R. Birringer, R. Strauß, and H. Gleiter, *Acta Metall.* **37**, 2485 (1989).
- ¹³H. Gleiter, *Phys. Status Solidi B* **172**, 41 (1992).
- ¹⁴C. L. Liu and S. J. Plimpton, *Phys. Rev. B* **51**, 4523 (1995).
- ¹⁵M. R. Sørensen, Y. Mishin, and A. F. Voter, *Phys. Rev. B* **62**, 3658 (2000).
- ¹⁶A. Suzuki and Y. Mishin, *Interface Sci.* **11**, 131 (2003).
- ¹⁷A. Suzuki and Y. Mishin, *J. Mater. Sci.* **40**, 3155 (2005).
- ¹⁸T. Frolov and Y. Mishin, *Phys. Rev. B* **79**, 174110 (2009).
- ¹⁹Y. Mishin, M. Asta, and J. Li, *Acta Mater.* **58**, 1117 (2010).
- ²⁰C. Deng and C. A. Schuh, *Phys. Rev. B* **84**, 214102 (2011).
- ²¹M. I. Mendelev and Y. Mishin, *Phys. Rev. B* **80**, 144111 (2009).
- ²²D. V. Bachurin and P. Gumbsch, *Phys. Rev. B* **85**, 085407 (2012).
- ²³G. J. J. Gao, Y. J. Wang, and S. Ogata, *Comput. Mater. Sci.* **79**, 56 (2013).
- ²⁴Y. Mishin, M. J. Mehl, D. A. Papaconstantopoulos, A. F. Voter, and J. D. Kress, *Phys. Rev. B* **63**, 224106 (2001).
- ²⁵S. Plimpton, *J. Comput. Phys.* **117**, 1 (1995).
- ²⁶S. Nosé, *Mol. Phys.* **52**, 255 (1984); W. G. Hoover, *Phys. Rev. A* **31**, 1695 (1985).
- ²⁷M. Parrinello and A. Rahman, *J. Appl. Phys.* **52**, 7182 (1981).
- ²⁸E. W. Hart, *Acta Metall.* **5**, 597 (1957).
- ²⁹E. A. Stern, R. W. Siegel, M. Newville, P. G. Sanders, and D. Haskel, *Phys. Rev. Lett.* **75**, 3874 (1995).
- ³⁰J. C. Maxwell-Garnett, *Philos. Trans. R. Soc. London* **203**, 385 (1904).
- ³¹J. Li, *Modell. Simul. Mater. Sci. Eng.* **11**, 173 (2003).
- ³²See Supplemental Material at <http://link.aps.org/supplemental/10.1103/PhysRevB.88.115413> for triple junction diffusion channels, and 3D view of the fast-diffusion channels in NC copper.
- ³³I. V. Belova and G. E. Murch, *J. Phys. Chem. Solids* **64**, 873 (2003).
- ³⁴Y. Chen and C. A. Schuh, *J. Appl. Phys.* **101**, 063524 (2007).
- ³⁵Y. Amouyal, S. V. Divinski, L. Klingner, and E. Rabkin, *Acta Mater.* **56**, 5500 (2008).
- ³⁶H. L. Wang, Z. B. Wang, and K. Lu, *Acta Mater.* **59**, 1818 (2011).
- ³⁷S. Divinski, J. Ribbe, G. Schmitz, and C. Herzig, *Acta Mater.* **55**, 3337 (2007).
- ³⁸Y. Chen and C. A. Schuh, *Scr. Mater.* **57**, 253 (2007).
- ³⁹S. V. Divinski, H. Edelhoff, and S. Prokofjev, *Phys. Rev. B* **85**, 144104 (2012).
- ⁴⁰M. Mantina, Y. Wang, R. Arroyave, L. Q. Chen, Z. K. Liu, and C. Wolverton, *Phys. Rev. Lett.* **100**, 215901 (2008).
- ⁴¹V. Milman, M. C. Payne, V. Heine, R. J. Needs, J. S. Lin, and M. H. Lee, *Phys. Rev. Lett.* **70**, 2928 (1993).
- ⁴²Y. J. Wang, A. Ishii, and S. Ogata, *Phys. Rev. B* **84**, 224102 (2011).
- ⁴³Y. J. Wang, A. Ishii, and S. Ogata, *Mater. Trans.* **53**, 156 (2012).
- ⁴⁴Y. J. Wang, A. Ishii, and S. Ogata, *Acta Mater.* **61**, 3866 (2013).